The Development Of Vehicle Dynamics Model For Dangerous Driving Behavior

ShuanFeng Zhao [1*], Guo Wei[1]

School of Mechanical Engineering, Xi'an university of Science and Technology, Xi'an, RR china.

Abstract

The vehicle dynamics model is based on models of the handling dynamics and the dynamic model of vehicle running status. Through online adaptation of the driver model parameter and some physical factors, which relate to the driver dangerous driving behavior, the driver and vehicle dynamic united model will describe vehicle running status of dangerous driving. Whether vehicle dynamics is accurate depends on appropriate tire model particularly in the study of maneuverability and stability of the vehicle. Due to the Semi-empirical tire model (Magic formula) does not reveals the relationship of the tire contact patch area, longitudinal force, lateral force and torque back positive. So it is necessary to establish a new tire model. A lattice spring model for vehicle tire is developed to overcome inherent weaknesses of traditional tire model, no describe vehicle dynamic characteristics under limit conditions caused by the emergency response and extreme operating of the driver. The developed vehicle dynamics model with dangerous driving behavior is verified from a long time fatigue driving test, in which the evolution of the fatigue of the driver was simulated.

Keywords: THE VEHICLE DYNAMICS MODEL, DRIVING BEHAVIOR, DISCRETE SPRING CONNECTION

1. Introduction

The transportation safety becomes an extremely important part in scientific research. Road traffic system, which integrates human, vehicles, roads, environment and other complex factors, is of high complexity, time-dependence and randomicity. The driver is the core factor of the driver-vehicle close-loop system and the source of traffic accident. The study is helpful to understand the driver's behavior under emergency and to provide basis for the driver safety management. On the surface, the traffic accident is an accidental emergent phenomenon, but its essence is an instability phenomenon of the driver-vehicle-environment closed-loop system caused by not able to respond to unforeseen circumstances in the driving.

Indiana University scientists' Research has shown that about 90 percent of the malignant traffic accidents related to the driver behavior [1], through a questionnaire survey to a large number of legacy traffic accident collision track, vehicle remains such evidence and survivors. The relevant researches scientists have come to similar conclusions [2].

Dangerous driving behavior mainly include two categories: one category is the mental state of danger, for example: the driver fatigue driving, drunk driving and drug driving. The other category is dangerous driving behavior, such as: speeding, severe overload. The first kind of dangerous behavior is the driver's own state of mind in the shrunken state, second types of driving behavior is subjective intentional behavior. Outside the driver's mental state obviously is not obvious in performance, and this behavior is difficult and hot spot in driver behavior surveillance. The

external performance obviously the driver's mental state is not obvious.

The driver is the core of the driver-vehicle-road closed-loop driving system. The driver controls the steering wheel, brake, accelerator, and clutch to make the vehicle forward according to a predetermined path. The driver's response time will extend if the driver is fatigue, listlessness, lack of concentration. These features lie in the running state of the vehicle data.

According to the closed-loop model of vehicle driving process of driving is divided to three parts, Perception; decision; operations. Figure 1 starts that process for us here.

From figure 1 we can see that if we get the vehicle condition data change caused by the driver's mental state changes, we must establish to a new vehicle dynamic model to meet the driver emergency operations.

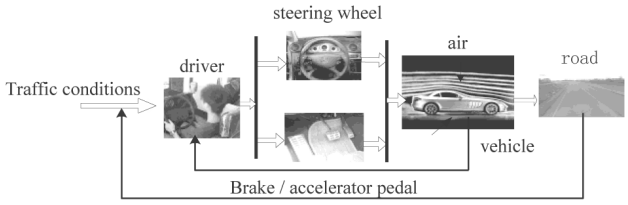

Figure 1. The driving process

2. The Vehicle Dynamic Model

2.1. The dynamic model of vehicle

The dynamic model of vehicle is the mathematical model reflecting the maneuverability and driving characteristics of the vehicle, is a measure of the virtual driving system based on the virtual manipulation of the authenticity of the important.The most classic model is a 7 degree of freedom two wheel model that can reflect the performance of the vehicle operator including the lateral movement and yaw movement[3]. The model is focused on the main performance of the vehicle and the number of model parameters is reduced to the minimum, especially the model can find the analytical solution. Scholars from different countries have established a number of complex vehicle models when computer appear, such as the Malaysian scholar Setia Wan, JD's 14 degrees of freedom model[4]. Complex model can describe the nonlinear characteristics of the vehicle and more precise movement of the dynamic response of the vehicle, but the determination of its parameters should be based on the experiment or man-made method instead of through fitting parameters, resulting in certain error affect the accuracy of the models. According to the risk state driving state of vehicle traffic simulation model of reality, simplifying the vehicle to eight degrees of freedom model, the eight degrees of freedom are: vertical translational motion of the vehicle, horizontally translational motion and around the Z axis horizontal pendulum movement three degrees of freedom and four wheel rotational degree of freedom and a front wheel steering degrees of freedom. The force analysis is shown in figure 2.

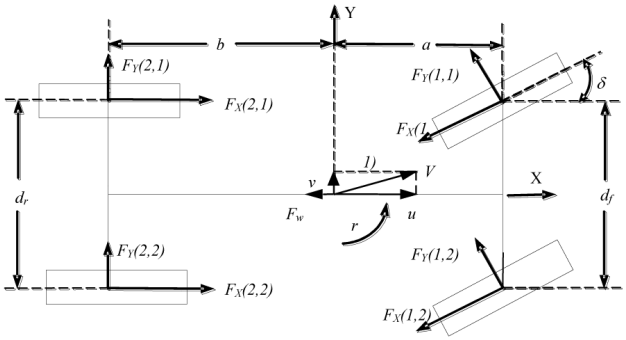

Figure 2. The motion and force diagram of vehicle model with eight degrees of freedom

V is velocity of the vehicle; u is the velocity component of V along the X axis; v is the velocity component of V along the Y-axis; β is the sideslip angle of the vehicle ; ω_r is vehicle yawing angular velocity; δ is the front wheel Angle; F_x is the longitudinal force, F_y is lateral adhesive force; a is the distance from the center of mass to front axle. b is the distance from the vehicle mass center to the rear axle; d_f, d_r is the front tracks and rear tracks respectively.

2.2. The vehicle centroid of three degrees of freedom kinematic differential equations

$$Ma_x = (F_X(1,1)+F_X(1,2))\cos\delta - (F_Y(1,1)+F_Y(1,2))\sin\delta - F_f - F_w \quad (1)$$

$$Ma_y = (F_Y(1,1)+F_Y(1,2))\cos\delta - (F_X(1,1)+F_X(1,2))\sin\delta + F_Y(2,1)+F_Y(2,2) \quad (2)$$

$$I_z\cdot\dot{\omega}_r = a\cdot(F_Y(1,1)+F_Y(2,2))\cdot\cos\delta + a\cdot(F_X(1,1)+F_X(1,2))\cdot\sin\delta - b\cdot(F_Y(2,1)+F_Y(2,2)) - 0.5\cdot D_f\cdot(F_X(1,1)-F_X(1,2))\cdot\cos\delta + 0.5\cdot D_f(F_Y(1,1)-F_Y(1,2)\cdot\sin\delta \quad (3)$$

$$F_w = C_d\cdot A\cdot V^2/21.15 \quad (4)$$

$$F_f = Mgf_0(1+V^2/19440) \quad (5)$$

M is the overall quality of the vehicle; I_z is the inertia of vehicle rotation around oz-axis; F_f is rolling resistance force; F_w is the wind resistance force; A is vehicle windward area; g is the gravitational acceleration; f is the tire rolling resistance coefficient; C_d is the wind resistance coefficient.

2.3. The vehicle wheels kinematics differential equations

The torque of vehicle engine drives the wheel by the transmission system. From figure 3 we can get the kinematics differential equation of vehicle four wheels:

$$I_w \cdot \dot{\omega}(1,1) = T_d(1) - F_X(1,1) \cdot R - M_f(1,1) - T_b(1,1) \quad (6)$$

$$I_w \cdot \dot{\omega}(1,2) = T_d(2) - F_X(1,2) \cdot R - M_f(1,2) - T_b(1,2) \quad (7)$$

$$I_w \cdot \dot{\omega}(2,1) = -F_X(2,1) \cdot R - M_f(2,1) - T_b(2,1) \quad (8)$$

$$I_w \cdot \dot{\omega}(2,2) = -F_X(2,2) \cdot R - M_f(2,2) - T_b(2,2) \quad (9)$$

$\omega(i,j)$ is the wheel angular velocity; T_d is the driving torque of transmission shaft; M_f is the wheel rolling resistance torque; T_b is the driving wheel braking torque/N·m; R is the radius of the tire.

Where in the drive torque distribution on the drive wheels can be obtained from the model of the vehicle driveline [5] The result is:

$$T_d(1) = T_d(2) = \frac{2I_w \eta i_g i_0 T_e}{4I_w + 2C} - \frac{C}{4I_w + 2C}\left(F_X(1,1) \cdot R + M_f(1,1) + T_b(1,1)\right) - \frac{C}{4I_w + 2C}\left(F_X(1,2) \cdot R + M_f(1,2) + T_b(1,2)\right) \quad (10)$$

$$C = i_g^2 \cdot i_0^2 \cdot I_e + i_0^2 \cdot I_g + I_0 \quad (11)$$

i_g is the transmission ratio; i_0 is the main reducer's gear radio; I_e is the inertia of the engine; I_g is the inertia of the transmission gears; I_0 is the inertia of differential; T_e is the engine output torque; η is the transmission efficiency; $T_d(1), T_d(2)$ is the driving torque on the left and right wheel respectively.

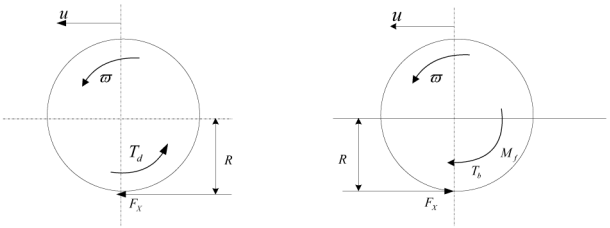

(a) Driving wheel (b) Engaged wheel

Figure 3. Force analysis

3. Tire model based on discrete spring connection

3.1. The state of tire model research

The vertical force, longitudinal force, lateral force, aligning torque, which has an important effect on vehicle ride comfort, handling stability[6]. Due to the nonlinearity of tire with the complexity structure and dynamic performance, it is the key to establish the simple and practical tire model for the vehicle running status simulation.

The current existence of the tire model consists of experience - semi-empirical model, physical model, the finite element model. experience - semi-empirical model is mainly aimed at a specific characteristics of tires, empirical formula obtained by fitting the test data, the current widely used formulas have Magic formula and Konghui Guo academician's, in Jilin university, uniform tire semi-empirical model of description six component characteristics based on exponential function tire[7-8]. The model requires a great deal of test data of the carcass, seem lack of flexible in application, in the simulation experiments didn't involve various kinds of working condition of the limit of reliability is insufficient.

Physical tire model[9] is based on the mechanical properties of the tire through mathematical derivation and form with a mathematical model of the analytic expression of its advantages is the ability to explore the formation mechanism of tire properties, the disadvantage is that the precision of the model than experience semi-empirical model is poor.

Finite element model is based on a detailed description of the tire structure, including geometry and material properties, accurate modeling to analysis calculates the steady state and dynamic response of the tire, but contact with the ground model is relatively complex, unable to complete real-time computing, rarely used in vehicle dynamics simulation research, mainly used in tire design and manufacturing.

In order to study the driver's operation behavior and the characteristics of the vehicle driving state data when the vehicle the driver woke with a start , we must make the tire model can reflect the extreme conditions[10] the stress distribution of the tire. Experience - semi-empirical tire model of traditional model parameters is more, Magic formula and parameters have clear physical meaning, but the model can't reflect the tire answered region length change of longitudinal force, side force and the influence of the back is the torque, and according to the formula parameters requires a lot of experimental data, it is difficult to be used for risk state under the working conditions of the limit of vehicle dynamics simulation.

3.2. Tire radial spring model

Tire radial spring model and ring model is physical model of the two kinds of typical. Radial spring model is independent of each other discrete spring is used to describe the tire characteristic[11]. Schmeitz

improved the radial spring deformation depends on the next spring[14]. Ring model according to the tire is made up of high strength and circumferential layout with beam and layout of the radial tire body; it will tire on the basis of simplified as elastic ring is analyzed. Rim and tire is connected with radial, tangential and lateral spring.

In 2008, Seongho Kim based on ring model based on the relevant deduction method of radial spring model, put forward an improved discrete multi degree of freedom spring ring beam tire model. The tire model can estimate the tire and the ground contact pressure, overcome the Magic formula tire model can not correctly reflect the tire area length change of longitudinal force, side force and the influence of the back is the torque [12] and the parameters of the need to identify less than Magic formula tire model and easy to implement, very suitable for simulating vehicle operating under extreme working conditions of nonlinear dynamic characteristics.

Vehicle dynamics in the process of building model with the tire model as shown in figure 4, model consists of rigid rings, six degree of freedom spring/damper unit, static ring beam, and the radial direction of the compensation spring of four parts. Rigid rings mainly reflects the inertia characteristics of the tire, rim and tires of 6 degree of freedom spring/damper unit mainly in order to reflect the tire transient characteristics of the first-order modal, static ring beam reflected through a series of the radial tire radial residual stiffness spring connected to rigid rings, mainly in order to reflect the tire circumferential layout with the radial deformation of beam.

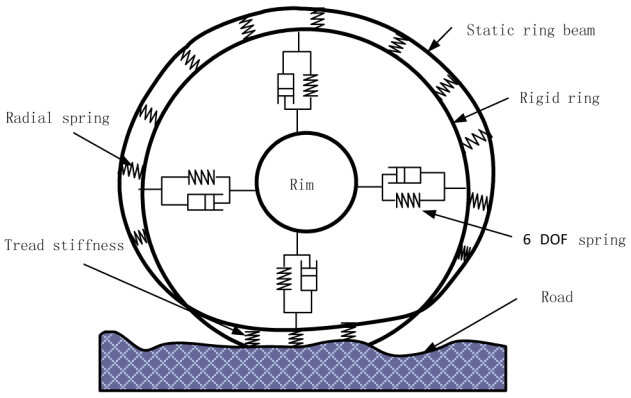

Figure 4. The tire model based on discrete spring

The dynamic equations can be solved by the contact pressure distribution and each infinitesimal element of the contact and deduce all kinds of tire mechanical properties under the pure condition. Tire longitudinal force and lateral force calculation formula is:

$$F_X = \int \sigma_X \mathrm{d}A$$
$$F_Y = \int \sigma_Y \mathrm{d}A \quad (11)$$

In the equation:

F_X, F_Y is tire longitudinal and lateral forces respectively, σ_x, σ_y respectively for the tire contact area of the longitudinal shear stress and the tangential shear stress , A for the area of tire contact with the ground mark, their specific calculation formula is as follows:

$$\sigma_x = \begin{cases} k(t)_{\xi_C} \cdot u(t)\xi_C & if\ k(t)_{\xi_C} \cdot u(t)_{\xi_C} \le \mu_{\xi_C} \cdot p \\ \mu_{\xi_C} \cdot p & f\ k(t)_{\xi_C} \cdot u(t)_{\xi_C} > \mu_{\xi_C} \cdot p \end{cases} \quad (12)$$

$$\sigma_Y = \begin{cases} k(t)_{\eta_C} \cdot u(t)_{\eta_C} & if\ k(t)_{\eta_C} \cdot u(t)_{\eta_C} \le \mu_{\eta_C} \cdot p \\ \mu_{\eta_C} \cdot p & if\ k(t)_{\eta_C} \cdot u(t)_{\eta_C} > \mu_{\eta_C} \cdot p \end{cases} \quad (13)$$

In the equation:

$k(t)_{\xi_C}, k(t)_{\eta_C}$ for the tread of the brush body longitudinal and lateral stiffness($\mathrm{N/m^3}$), $u(t)_{\xi_C}, u(t)_{\eta_C}$ for longitudinal and lateral deformation, $\mu_{\xi_C}, \mu_{\eta_C}$ for longitudinal and lateral friction coefficient, p for tire pressure in contact with the road surface($\mathrm{N/m^2}$).

The pressure distribution under the action of vertical load is the key to solve the equation 11. Gim G and Nikravesh P. Adeduced the contact pressure distribution under arbitrary vertical loading by the analysis of tire contact area radial deformation[14].

Figure 5 is a schematic diagram of deformation zone with tire and irregular ground contact; it can be seen from the figure, the contact point deformation u_r along the diameter consists of two parts: tire crown deformation and tire band deformation.

$$u_r = u_{(t)r} + u_{(b)r} \quad (14)$$

The any point pressure in tire corwn deformation zone can be expressed as the function of tread stiffness, namely:

$$p = -k_{(t)r}(u_r - u_{(b)r}) \quad (15)$$

In the equation:

$k_{(t)r}$ is the radial stiffness of tire crown unit area ($\mathrm{N/m^3}$), u_r is the tire strain along the radial direction, $u(b)r$ is band strain in tire.

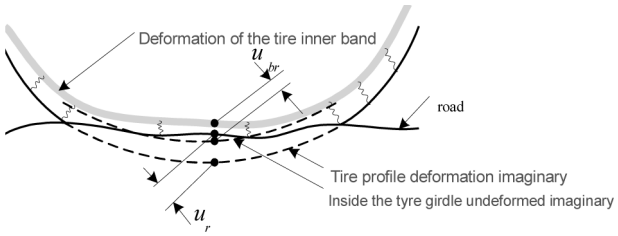

Figure 5. tires - surface contact deformation

If the tire circumferential direction is divided into N unit, according to the theory of elastic mechanics, the *ith* cell strain in band can be obtained by the follow equation:

$$u^i_{(b)r} = \sum_j^N p_j \bar{u}^{ij}_{(b)r} \Delta A^j \tag{16}$$

In the equation:

N is the unit number along the tire circumferential direction, p^j is *jth* unit contact pressure, $\bar{u}^{ij}_{(b)r}$ is *ith* radial strain caused by the unit force, ΔA^j is *jth* unit area. If the tread were divided into equal size units, $\Delta A^j = \Delta A$, the matrix format equation is written as the follow by put the formula 14 into 15.

$$\begin{bmatrix} (-\frac{1}{k_{(t)r}\Delta A} + \bar{u}^{11}_{(b)r}) & & \bar{u}^{1N}_{(b)r} \\ & \ddots & \\ \bar{u}^{N1}_{(b)r} & & (-\frac{1}{k_{(t)r}\Delta A} + \bar{u}^{NN}_{(b)r}) \end{bmatrix} \begin{Bmatrix} u^1_{b(r)} \\ \vdots \\ u^N_{b(r)} \end{Bmatrix} = \begin{Bmatrix} u^1_r \bar{u}^{11}_{(b)r} + \ldots + u^N_r \bar{u}^{1N}_{(b)r} \\ \vdots \\ u^1_r \bar{u}^{N1}_{(b)r} + \ldots + u^N_r \bar{u}^{NN}_{(b)r} \end{Bmatrix} \tag{17}$$

A tire band strain $u^i_{u(b)r}$ can be solved equations (17), so contact pressure of tire and road can be calculated by formula15. It is worth noting that this method do not need to be on the geometric shape of any assumptions, can apply any uneven road surface.

The tire was divided into N_ϕ and N_η units along the circumference and diameter direction. The meaning $\bar{u}^{ij}_{(b)r}$ is *ith* unit deformation when *jth* unit load on its.

The tires/road contact deformation is shown in figure 6, the deformation expression $\bar{u}_{(b)r}(\phi,\eta;\phi_p,\eta_p)$ along a belted tire radial direction under unit load is written as follows

$$\bar{u}_{(b)r}(\phi,\eta;\phi_p,\eta_p) \approx \bar{u}_{(b)r\phi}(\phi,\phi_p)\cdot\bar{u}_{(b)r\eta}(\eta,\eta_p) \tag{18}$$

In the equation:

$$\begin{aligned}\bar{u}_{(b)r\phi}(\phi,\phi_p) = \bar{C}_0 + \bar{C}_1\cosh(\alpha\cdot(\phi-\phi_p))\cos(\beta\cdot(\phi-\phi_p)) \\ + \bar{C}_4\sinh(\alpha\cdot(\phi-\phi_p))\sin(\beta\cdot(\phi-\phi_p))\end{aligned} \tag{19}$$

$$\begin{aligned}\bar{u}_{(b)r\eta}(\eta,\eta_p) = e^{-\lambda_{r\eta}|\eta-\eta_p|}\cos(\lambda_{r\eta}\cdot|\eta-\eta_p|) \\ + e^{-\lambda_{r\eta}|\eta-\eta_p|}\cos(\lambda_{r\eta}\cdot|\eta-\eta_p|)\end{aligned} \tag{20}$$

$$\bar{C}_0 = \frac{R^3}{2EI_{r\phi}\pi\lambda^2_{r\phi}} \tag{21}$$

$$\bar{C}_1 = \frac{R^3(\alpha\cosh(\pi\alpha)\sin(\pi\beta)+\beta\cos(\pi\beta)\sinh(\pi\alpha)}{2EI_{r\phi}\pi\alpha\beta(\alpha^2+\beta^2)(\cos(2\pi\beta)-\cosh(2\pi\alpha))} \tag{22}$$

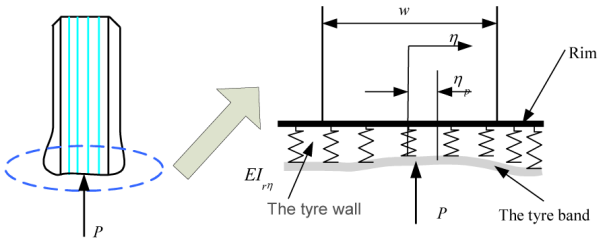

Figure 6. tires - road surface contact

$$\bar{C}_4 = \frac{R^3(\beta\cosh(\pi\alpha)\sin(\pi\beta)-\alpha\cos(\pi\beta)\sinh(\pi\alpha)}{2EI_{r\phi}\pi\alpha\beta(\alpha^2+\beta^2)(\cos(2\pi\beta)-\cosh(2\pi\alpha))} \tag{23}$$

$$\alpha = \sqrt{\frac{\lambda_{r\phi}-1}{2}} \quad and \quad \beta = \sqrt{\frac{\lambda_{r\phi}+1}{2}} \tag{24}$$

$$\lambda_{r\phi} = \sqrt{\frac{R^4 k_{r\phi}}{EI_{r\phi}}+1} \tag{25}$$

$$\lambda_{r\eta} = \sqrt[4]{\frac{k_{r\eta}}{4EI_{r\eta}}+1} \tag{26}$$

$$EI_{r\eta} = \frac{2\pi R}{w}EI_{r\phi} \tag{27}$$

$$k_{(t)\eta c} = \frac{C_a}{\int_A \hat{\xi}\mathrm{d}A} \tag{28}$$

$$k_{(t)\xi c} = \frac{C_s}{\int_A \hat{\xi}\mathrm{d}A} \tag{29}$$

R is the effective diameter of the tire, $EI_{r\phi}, EI_{r\eta}$ are the ring beam in radial and transverse bending strength, $k_{(t)r}, k_{(t)\eta c}, k_{(t)\xi c}$ respectively tire radial stiffness, the lateral stiffness of the per unit area, lateral stiffness, C_a, C_s respectively tire cornering stiffness, braking stiffness.

4. Simulation examples

Take 205/45R16, for instance, carries on the simulation analysis. The geometric parameters of tire: diameter $R = 0.2949m$, the breadth of tyre $w = 0.15m$, the mass of tyre $m = 8.365kg$, The moment of inertia $I_{xx} = I_{zz} = 0.4578\ \mathrm{kg\cdot m^2}$, $I_{yy} = 0.728\ \mathrm{kg\cdot m^2}$ The distribution of the contact pressure of the type parameters required is shown in table1, $\Delta = R - R_l$ in the list, where R_l is a measure of the radius from tire loading surface to the center of the tire.

Table 1. Tire parameter list

$EI_{r\phi}$ / N·m^2	$k_{(t)r}$ / N·m^{-3}	$k_{r\phi}$ / N·m^{-3}
13.049	1.4567×10^8	$(1.5146\times10^6)e^{-12.6921\Delta}$

Figure 7 shows that the model for the 205/45R16 tire effective diameter and length of contact line of the curve in the different load after load.

According to the specific numerical graph7, we can determine the radial residual stiffness values under different loads.

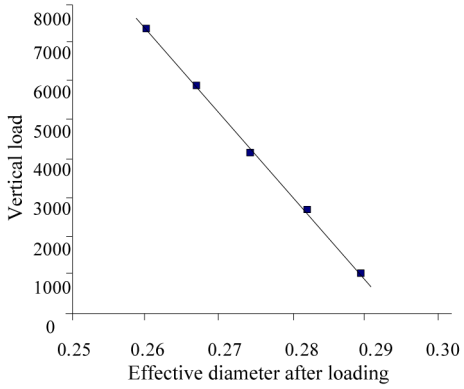

(a) Vertical load

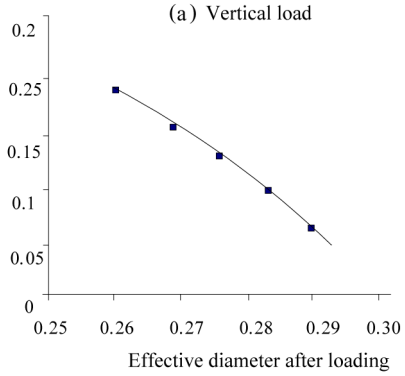

(b) The length of the contact line

Figure 7. tires - road surface contact

The tire circumferential and lateral was divided into 100 and 20 units when the tire geometry parameters, stiffness parameters, load size is determined.

The exact values of parameters $\overline{u}^{ij}_{(b)r}$ can be calculated by the formula 13 and 14. The belt deformations $u^{i}_{u(b)r}$ in tire are obtained by solving linear system of equations listed in equation 17. And we can figure out the contact pressure distribution by the equation 18, tire contact pressure and its distribution under different loads calculation results as shown in figure 8.

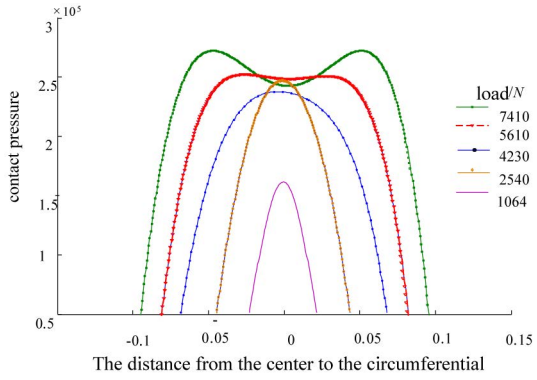

Figure 8. Tire - road contact pressure distribution

After the distribution of tire-road contact pressure p and deformation $u(t)$ is obtained, the tire lateral force F_X and lateral force F_Y can be computed by equation 10.

The relations amount longitudinal and transverse friction coefficient $\mu_{\xi_C}, \mu_{\eta_C}$, slip rate and slip angle can be expressed equation 30 and 31

$$\mu_{\xi c} = \hat{\mu}^{(s)}_{\xi c} + \left(\hat{\mu}^{(0)}_{\xi c} - \hat{\mu}^{(s)}_{\xi c}\right) \sec h\left(\frac{A_{\mu 1} \tanh\left(|s|\right)}{1-|s|}\right) \quad (30)$$

$$\mu_{\eta c} = \hat{\mu}^{(s)}_{\eta c} + \left(\hat{\mu}^{(0)}_{\eta c} - \hat{\mu}^{(s)}_{\eta c}\right) \sec h\left(\frac{B_{\mu 1} \tanh\left(|\tan\alpha|\right)}{1-|\tan\alpha|}\right) \quad (31)$$

where:

s is slip rate, a is tire slip angle, $\hat{\mu}^{(s)}_{\xi c}, \hat{\mu}^{(s)}_{\eta c}$ are transverse / lateral friction coefficient when the limit slip, $\hat{\mu}^{(s)}_{\xi c}$ $\hat{\mu}^{(s)}_{\eta c}$ are transverse / lateral static friction coefficient when the limit slip, $A_{\mu 1}, B_{\mu 1}$, are shape influence factor of friction coefficient function, its value is calibrated by the experiment data.

The value of friction coefficient shown in table 2 by consults the relevant manuals.

Table 2. Tire friction coefficient

$\hat{\mu}^{(s)}_{\xi c}$	$\hat{\mu}^{(s)}_{\eta c}$	$\hat{\mu}^{(s)}_{\xi c}$	$\hat{\mu}^{(s)}_{\eta c}$	$A_{\mu 1}$	$B_{\mu 1}$
1.2	1.2	1.0	1.0	3.0	3.0

Discrete spring tire model simulation results in various running conditions shown in figure 9.

Figure 9 (a) is a vertical loads under different tire side force with the tire side slip angle curve in pure condition, Figure 9(b) is slip rate curve under different loads in pure lateral slip condition. Figure 9 (c, d) are lateral / longitudinal force change with the slip ratio under the curve at the different angle-working.

4.1. Vehicle Dynamics Simulation Example

In order to verify the reasonableness and accuracy of the established model, a circular runway acceleration test as a simulation example and the value which the vehicle model parameters as shown in Table 3.

Table 3. Simulation parameters of Vehicle Model

M / kg	m_w / kg	I_z / kg · m^2	A / m^2
1296	37	1399	2
a / m	b / m	d_f / m	d_r / m
1.25	1.32	1.405	1.399

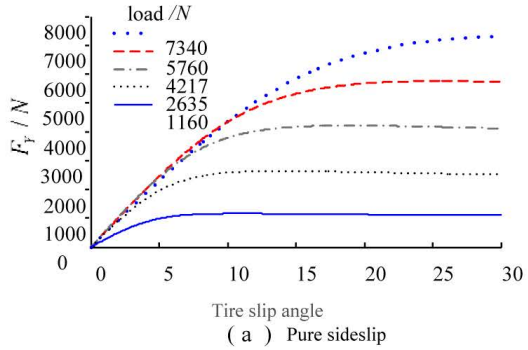

(a) Pure sideslip

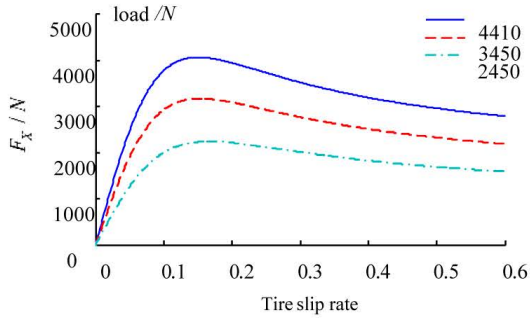

(b) Pure cross slip

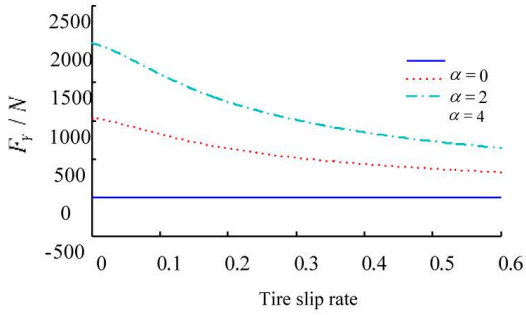

(c) Slip ratio curve

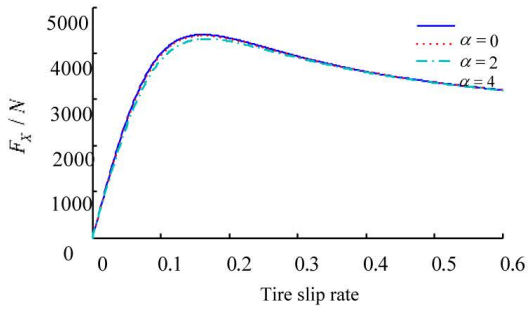

(d) Longitudinal force varies slip rate

Figure 9. The results of the tire lateral force / longitudinal force

When the vehicle is accelerated circular motion in the annular runway, the relationship between the front wheel steering angle α and radius R is:

$$R_c = \frac{d_f}{\delta - (\alpha_1 - \alpha_2)} \tag{32}$$

Where:

d_f is the wheelbase, δ is a front wheel steering angle, α_1, α_2 are the absolute value of the front wheel and the rear wheel side slip angles.

The vehicle should have understeering characteristics in regulation for design of safety regulations for vehicle, that is to say the $(\alpha_1 - \alpha_2)$ will increase with the increase of lateral acceleration.

Figure 10 is the result of simulation acceleration test annular runway, in which the vehicle model using the parameters listed in table 3. From Figure 10 (a) we can be seen the vehicle motion trajectory is a closed circular and consistent with the target trajectory, it proved that the vehicle dynamic model is convergent.

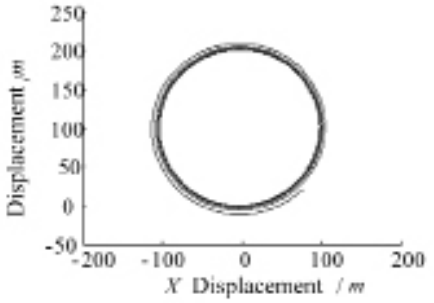

(a) The centroid trajectory

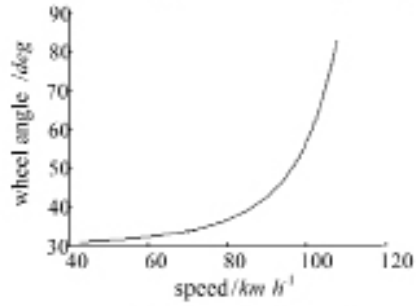

(b) Steering characteristics

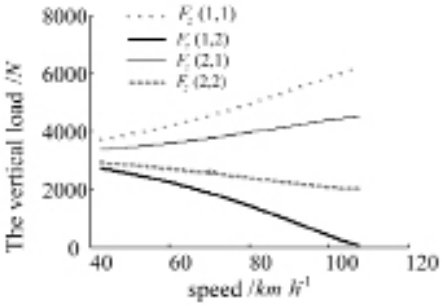

(c) The vertical load

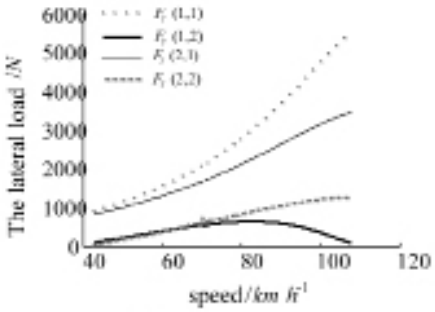

(d) The lateral load

Figure 10. The simulation results of circular runway speeding

As can be seen from Figure 10 (b), if the vehicle remains in a circular motion then the front wheel angle as the vehicle speed increases, it is consistent with the understeer characteristic described in equation 19. Figure 10(c,d) is the force of tire, it reveals the tire load during re-acceleration distribution: Vertical load suffered significant increase in the inside of the curve near the front wheel and in the corners during acceleration. The rules in accordance with the relevant to describe the vehicle theory, which indirectly proves the correctness of vehicle dynamics model built in the in the thesis and practical.

4.2. Fatigue state vehicle driving behavior simulation example

H. B. K. Boom and A. J. Mulder [16]research show that the mathematical properties of the human body fatigue can be describe by the sigmoid function, the relationship among the fatigue degree ,the neuronal response time and action reaction time were written as follows:

$$\begin{cases} \overline{t_d} = \ln(-\dfrac{N_t - 1}{N_t}) \cdot \dfrac{(t_{da} - t_{db})}{4} + \dfrac{t_{da} + t_{db}}{2} \\ \overline{T_h} = \ln(-\dfrac{N_t - 1}{N_t}) \cdot \dfrac{(T_{ha} - T_{hb})}{4} + \dfrac{T_{ha} + T_{hb}}{2} \end{cases} \quad (33)$$

N_t is Driver fatigue degree of t time, t_{da} is the upper limit of driver neuronal response time, t_{db} is the lower limit of driver neuronal response time, T_{ha} is the upper limit of driver action response time, T_{hb} is the lower limit of driver action response time.

The most important physical significance above expression is to establish the relationship among driver fatigue index, driver average action response time, driver average neuronal response time. According to the link of the variance of the driver model parameter and the driver attention, the probabilistic distribution parameters of the driver model were determined under the given fatigue index value. The relationship between the fatigue degree and the driver model parameters are obtained.

In order to analyze the rationality and applicability of proposed model, we chose two common types of road and utilize entire vehicle model of four degree of freedom to simulate closed loop system of «driver-vehicle-road".

Take the lane changing and round the corner as examples to study fatigue driving simulation analysis, and the corresponding distribution of attention in every link of the table 4.

Table 4. Distribution of steady attention on different driving state of the driver

The driving state	preview link	judgment link	action link
line	0.86	0.09	0.05
Lane changing	0.68	0.20	0.12
Intersection	0.56	0.21	0.23

Figure 11 is the simulation of double lane change maneuver results when the driver of continuous driving 2 hours (normal driving), 4 hours (slight fatigue), 8 hours (moderate fatigue) after.

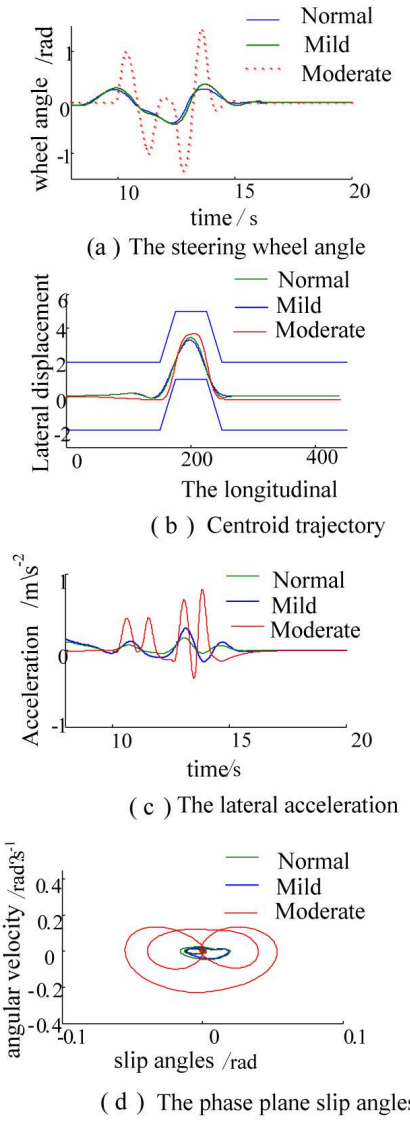

(a) The steering wheel angle

(b) Centroid trajectory

(c) The lateral acceleration

(d) The phase plane slip angles

Figure 11. The double lane change

Figure 11 to show the steering wheel angle, center of mass trajectory, lateral acceleration, side slip angle side angle velocity of the phase plane curve. The side slip angle and side slip angle velocity phase plane is an index to reflect the vehicle stability margin [15], seen from the chart with the prolonged driving time, phase plane closed area becomes larger, the stability margin to reduce vehicle.

Description of simulation in double lane change road: the slowly varying curvature case, simulation results that this model can be used to simulation driving state of vehicle under the driver fatigue.

The normal driving, mild fatigue driving and moderate fatigue driving vehicle running simulation results show in the figure 12. The experienced drivers makes the vehicle steering, and then slowly its return at the right angle corner.

The simulation results of wheel angle is consistent with the actual operation of the driver as a result, the correctness of constructed models is proved.

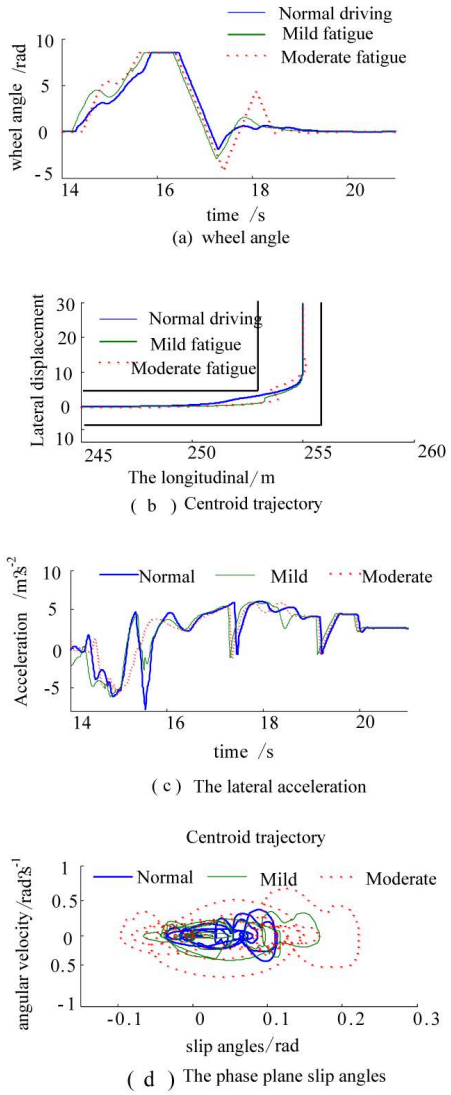

Figure 12. round the corner

5. Conclusions

It is known that the driving characteristics during the risk driving are dynamic and the driver model is also time-varying under different stages in the close-loop system of driver, vehicle and road. It causes the time-varying problem in risk driving diagnosis. To tackle this problem, A lattice spring model for vehicle tire is developed to overcome inherent weaknesses of traditional tire model. The finished work is as follows:

1) A simulation model of Vehicle running status is developed, whose input is risk driving indicators. A model on shifting of the driver's attention is developed to study the relationship between driving behavior and parameters in the driver model. A lattice spring model for vehicle tire is developed to overcome inherent weaknesses of traditional tire model, no reflect vehicle dynamic characteristics under limit conditions caused by the emergency response and extreme operating of the driver. The developed close-loop risk driving model is verified from a long time fatigue driving test, in which the time evolution of the fatigue process of the driver was simulated.

2) Driver fatigue as an example to verify the vehicle dynamics model for dangerous diving behavior is the correctness of simulation of vehicle running state. On the basis of the driver model parameters inherent characteristics and the physical meaning of driver behavior analysis, the model be used to driver fatigue driving dynamic evolution characteristics.

Acknowledgment

This work is supported by National Natural Science Foundation of China (Project 51305339) and Natural science basic research plan in shaanxi province of china(Program No 2013JM7022)

References

1. Janicak C, A. Differences in relative risks for fatal occupational highway transportation accidents. Journal of Safety Research, 2003;34 (5), p.p 539-545.
2. Yannis G, Golias J and Papadimitriou E.. Accident risk of foreign drivers in various road environments. Journal of Safety Research, 2007;38 (4), p.p 471-480.
3. Shiiba Taichi and Suda Yoshihiro. Development of driving simulator with full vehicle model of multibody dynamics. JSAE Review, 2002;23 (2), p.p 223-230.
4. Setiawan Joga Dharma, Safarudin Mochamad and Singh Amrik. Modeling, simulation and validation of 14 DOF full vehicle model. IEEE Computer Society, 2009;Indonesia: Bandung.
5. ChengBao Zhang. Theoretical research on vehicle anti-slip regulation and vehicle dynamics. Dissertation.2000; Tongji University. Shanghai.
6. Dihua Guan, Chengjian Fan.. A summary of the tire model for vehicle dynamics simula-

tion on uneven road . *A*utomotive engineering, 2004;26 (2), p.p 162-167.
7. Guo K, Lu D, Chen S-K, et al.. The UniTire model: A nonlinear and non-steady -state tyre model for vehicle dynamics simulation. Vehicle System Dynamics, 2005;43 (SUPPL), p.p 341-358.
8. Guo K, Xu N, Lu D, et al. A Model for Combined Tire Cornering and Braking Forces with Anisotropic Tread and Carcass Stiffness. SAE International Journal of Commercial Vehicles,2011; 4 (1), p.p 84-95.
9. Zegelaar PWA, Gong S, Pacejka HB.. Tyre models for the study of in-plane dynamics. Vehicle System Dynamics, 1994;23 (SUPPL) p.p 578-590.
10. Besselink IJM, Pacejka HB, Schmeitz AJC, et al. The MF-Swift tyre model: Extending the Magic Formula with rigid ring dynamics and an enveloping model. Review of Automotive Engineering, 2005,26 (2) p.p 245-252.
11. Schmeitz AJC, Versteden WD.. Structure and parameterization of MF- swift, a magic formula-based rigid ring tire model. Tire Science and Technology, 2009, 37 (3) ,p.p 142-164.
14. Kim S, E.Nikravesh P, Gim G. A two-dimensional tire model on uneven roads for vehicle dynamic simulation. Vehicle System Dynamics, 2008;46 (10), p.p 913-930.
13. Pacejka HB, Sharp RS. Shear force development by pneumatic tyres in steady state conditions. A review of modelling aspects. Vehicle System Dynamics, 1991;20 (3-4), p.p 121-176.
14. Gim G, Nikravesh P.. A Three Dimensional Tire Model for Steady-State Simulations of Vehicles. SAE Technical Paper, 1993;doi: 10.4271/931913.
15. Yuxian Gai,QingDi Guo.. Research on vehicle dynamics stability . Journal of Harbin Institute of Technology, 2006,38 (12), p.p 2112-2116.
16. Boom HBK, Mulder AJ and Veltink PH. Fatigue during functional neuromuscular stimulation. ProgrBrain Res, 1993;97 (3), p.p 409-418.

A Fast and Robust Segmentation method for Liver Tumor

Hua Zou[1,2,*], Fu Lin[1], Lei Guo[1]

[1] *School of Computer, Wuhan University, Wuhan, Hubei, 430072, China*
[2] *Su zhou Institute of Wuhan University, Suzhou, Jiangsu,215123, China*

Abstract
To segment the liver tumor accurately, this paper proposes a segmentation method which combines relative fuzzy connectedness with level set method. First, liver tumor is roughly segmented using relative fuzzy connectedness. Second, the result of preliminary segmentation is as the initial contour of level set method. The accurate boundaries of liver tumor are then segmented using level set method. Last, an adaptive velocity evolution function is